JOURNAL OF GREEN COMPLEX ENGINEERING, 2026, Vol.4, No.1, 99~106
https://doi.org/10.59810/greenplexresearch.v4i1.286
e-ISSN 3025-9673

Downstream Amplification of Suspended-sediment Flux Outpaces Discharge Growth in the Mangottong River, Indonesia

Muhammad Scyroth Arianto*, Ilfan Muis, Andi Makbul Syamsuri, Fithriyah Arief Wangsa

Department of Water Resources Engineering, Faculty of Engineering, Universitas Muhammadiyah Makassar, Makassar, Indonesia

ABSTRACT

Suspended-sediment transport in small tropical rivers can change sharply over short distances because discharge, sediment availability, and cross-sectional mixing vary simultaneously. This study examined longitudinal changes in water discharge, suspended-sediment concentration (SSC), and instantaneous suspended-sediment flux along the Mangottong River, South Sulawesi, Indonesia. Five observations were available at each upstream, midstream, and downstream cross-section. Point discharges were verified from the field calculations, SSC was derived from laboratory dry-mass measurements, and section concentration was evaluated using discharge weighting. Suspended load was calculated as 0.0864CQ, with C in mg L^{-1} and Q in m^3 s^{-1}. Section discharge increased from 5.178 to 7.554 and 8.438 m^3 s^{-1}, whereas discharge-weighted SSC changed from 626.5 to 568.3 and 1,829.2 mg L^{-1}. Corresponding suspended loads were 280.3, 370.9, and 1,333.5 t d^{-1}. The downstream section therefore carried 4.76 times the upstream load while water discharge increased only 1.63-fold. The lower-reach amplification was driven primarily by sediment enrichment rather than discharge growth alone, demonstrating the value of discharge-weighted sampling for interpreting sparse river surveys.

ARTICLE HISTORY

Received June 20, 2026
Received in revised form July 25, 2026
Accepted August 20, 2026
Available online August 27, 2026.

KEYWORDS

suspended sediment; sediment flux; river discharge; discharge-weighted concentration; tropical river

1. Introduction

Rivers transfer sediment through a sequence of entrainment, suspension, deposition, and remobilization that is governed by both hydraulic energy and the availability of erodible material. In practical river engineering, the quantity of suspended material matters because it affects channel conveyance, intake performance, downstream shoaling, water quality, and the amount of fine sediment delivered to estuaries and coastal waters. The relation between discharge and suspended sediment, however, is rarely proportional over all flow conditions. Monitoring studies have shown that high flows can move a large share of annual sediment, while sediment exhaustion, antecedent conditions, and event timing can produce substantial departures from a single discharge–concentration relation [1-3].

This problem is particularly relevant in tropical catchments, where intense rainfall, seasonal changes in runoff, land disturbance, and rapid channel adjustment can produce large variations in suspended-sediment transport over relatively short distances. Field and modelling studies in tropical and monsoon-influenced rivers have reported marked seasonal and spatial differences in sediment production and downstream delivery [4,5]. Indonesian observations likewise show that flow structure and sediment distribution can vary across a cross-section and along a river reach, so a single point measurement may not represent the section as a whole [6,7].

Longitudinal changes also reflect sediment sources and temporary storage. Streambanks, tributaries, fine material stored on the bed, and disturbed floodplain surfaces can contribute different proportions of the transported sediment as drainage area increases. Sediment-budget studies have found that stream-corridor sources may become more important downstream and that neighbouring reaches can alternate between net sediment gain and loss [8,9]. At broader scales, specific sediment yield varies with topography, runoff, lithology, vegetation, and land use rather than with discharge alone [10]. Recent small-catchment work has also documented several-fold downstream increases in suspended transport where urbanisation and local sediment sources modify the hydro-sedimentary response [11], while comparative measurements in the Brahmaputra show that upstream and downstream sediment–water relations can be inconsistent even within the same river system [12].

These observations make the distinction between concentration and flux essential. Suspended-sediment concentration expresses mass per unit water volume, whereas sediment flux expresses mass transported through a cross-section per unit time. A high concentration at a low-discharge subsection may contribute less sediment mass than a moderate concentration within the main conveyance zone. Conversely, two sections with similar discharge can transport very different sediment loads if sediment availability differs. Section-scale interpretation therefore requires concentration to be combined with the amount of water represented by each sampling location. This principle is also reflected in modern monitoring practice. High-frequency optical and radiometric methods are increasingly used to capture rapid sediment variability [13,14], while sediment rating curves remain useful in data-scarce rivers but perform differently among sites and seasons [15,16].

CONTACT: Muhammad Scyroth Arianto reganzbugis@gmail.com Department of Water Resources Engineering, Faculty of Engineering, Universitas Muhammadiyah Makassar, Makassar, Indonesia

A further complication is that sediment transport responds to a sequence of flow states rather than to discharge magnitude in isolation. During rising stages, fresh material can be mobilised from hillslopes, banks, and channel margins; during recession, available fine sediment may become depleted even while discharge remains relatively high. This produces event-specific trajectories in the discharge–SSC relation and limits the value of interpreting a single concentration without its hydraulic context [2]. In data-scarce systems, this temporal uncertainty cannot be eliminated, but a physically consistent cross-sectional mass balance can still distinguish whether a measured load increase reflects more water, more sediment per unit water, or both.

Local hydraulic controls can further change the relation between flow and sediment movement. Recent experiments in the Journal of Green Complex Engineering show that modifying flow structure alters velocity, Froude regime, sediment retention, and scour response under controlled conditions. A beam-type sabo dam reduced debris transport efficiency as channel slope and flow intensity changed [17], while porous underwater deflectors reduced near-bed velocity and local scour around bridge-pier models [18,19]. Although these laboratory configurations differ from an unregulated natural river, they reinforce a relevant physical point: transport capacity and sediment mobilisation respond to local hydraulics, so river-scale sediment patterns cannot be inferred from discharge totals alone.

The Mangottong River in Sinjai Regency, South Sulawesi, provides a useful small-river case for examining this coupling. The sampled corridor extends from the Samaenre area of Sinjai Tengah toward the lower reach near Samataring, Sinjai Timur, over an interval of approximately 5 km. The river is important for local drainage and agricultural water management, and sediment accumulation has been a concern because reduced conveyance can compound flood and river-mouth problems. Field measurements were made at upstream, midstream, and downstream cross-sections, each represented by five point observations of hydraulic discharge and suspended sediment.

A review of the field calculations identified a practical issue that is common in manually processed hydrometric datasets: the reported downstream section total did not equal the sum of the five listed subsection discharges, and the unit used for sediment load was inconsistent with the stated conversion factor. Rather than carrying these discrepancies into the interpretation, the present analysis uses the explicitly reported point values, verifies section totals by summation, and calculates suspended-sediment flux with dimensional consistency. The purpose is to determine whether the observed downstream increase in suspended load is explained mainly by increasing water discharge or by a concurrent increase in sediment concentration. The working hypothesis is that sediment flux rises faster than discharge because the lower reach is enriched in suspended material. The analysis therefore compares longitudinal discharge ratios, discharge-weighted SSC, and integrated suspended load, while also examining lateral heterogeneity within each cross-section.

2. Methods

2.1 Study area and field observations

The study used field and laboratory observations from three cross-sections of the Mangottong River: upstream, midstream, and downstream. Five sampling points (P1–P5) were reported at each section. The field programme measured channel depth, cross-sectional geometry, flow velocity, and water discharge. Velocity observations were obtained with a Flowatch/current-meter approach and a float method. Water samples were collected for laboratory determination of suspended-sediment mass, and the reported sample volume was 1.5 L. The original survey also used an echo sounder for channel-depth measurements.

The analysis was restricted to values that were explicitly recoverable from the final field and laboratory calculations. This choice was necessary because some intermediate velocity averages and subsection areas were internally inconsistent. For the hydraulic dataset, the retained point discharges were 0.407, 1.026, 1.340, 1.616, and 0.789 $m^3\ s^{-1}$ upstream; 0.624, 1.300, 1.760, 2.460, and 1.410 $m^3\ s^{-1}$ midstream; and 0.672, 2.131, 1.676, 2.839, and 1.120 $m^3\ s^{-1}$ downstream. Section discharge was calculated as the sum of the five point values. This gives 8.438 $m^3\ s^{-1}$ downstream, rather than the 9.518 $m^3\ s^{-1}$ total written in the original worksheet.

2.2 Suspended-sediment concentration and load

Cross-sectional area was calculated by the trapezoidal rule, A = Σ[(h_i + h_(i+1))/2]Δx, where h_i and h_(i+1) are adjacent depth ordinates and Δx is the horizontal distance between them. With five ordinates per section, the channel width was divided into four equal intervals. This approach is mathematically transparent and directly reproducible from the recorded field values.

Laboratory SSC values retained for analysis were 266.6, 200.0, 466.6, 1,133.3, and 600.0 mg L^{-1} upstream; 400.0, 466.6, 533.3, 633.3, and 666.6 mg L^{-1} midstream; and 1,266.0, 1,400.0, 533.3, 2,666.6, and 2,800.0 mg L^{-1} downstream. These values were derived from dry sediment mass divided by sample volume. Because each point represented a different amount of water, section SSC was also expressed as a discharge-weighted concentration:

$$C_w = \frac{\sum Q_i C_i}{\sum Q_i}$$

where Qi is point discharge, Ci is point SSC, and Cw is the section-weighted concentration.

Instantaneous suspended-sediment load was calculated for each point from:

$$L_s = 0.0864\, CQ$$

where Ls is suspended load in t d^{-1}, C is SSC in mg L^{-1}, and Q is discharge in $m^3\ s^{-1}$. The factor 0.0864 follows directly from converting mg L^{-1} to g m^{-3} and seconds to days. Point loads were summed to obtain section load. These quantities describe transport during the sampled state; they are not annual sediment yield and they do not by themselves quantify deposition. A difference between downstream and upstream suspended loads is therefore interpreted as a longitudinal load gain, not as a sedimentation rate.

2.3 Data verification and statistical analysis

Descriptive statistics were calculated for point discharge, SSC, and point suspended load. Longitudinal differences in SSC were evaluated with a Kruskal–Wallis test because each section contained only five observations and downstream concentrations were strongly skewed. When the omnibus result was significant, pairwise Mann–Whitney comparisons were examined with Holm adjustment. The same omnibus test was applied to point load. Spearman rank correlation was used to assess the association between point discharge and SSC. The discharge–load correlation was treated only as descriptive because discharge is a term in the load equation. The analysis emphasised effect magnitude, longitudinal ratios, and section-integrated mass flux rather than relying on p values alone.

For quality control, every integrated quantity was recomputed from the retained point values. Arithmetic means were used only to describe the five sampled points, whereas section-scale transport was calculated from $\Sigma Q_i C_i$ so that each observation was weighted by the water volume it represented. This distinction is important because the downstream section contained both high- and low-SSC points. The section load is therefore not the product of the arithmetic mean SSC and total discharge; it is the sum of pointwise mass fluxes. Ratios were calculated from these integrated quantities: downstream-to-upstream discharge, downstream-to-upstream weighted SSC, and downstream-to-upstream suspended load. These ratios provide a direct test of the hypothesis that sediment enrichment amplifies transport beyond the effect of increasing water discharge.

2.4 Monitoring framework

Figure 1 shows the sampling framework used in the analysis. The diagram is schematic and does not imply unreported geographic coordinates or equal distances among P1–P5. In future monitoring, section placement and instrumentation should be tied to flood-prone and hydraulically representative locations. The value of integrating hydrological measurement structures with spatial vulnerability assessment has also been demonstrated for village-scale flood mitigation in Indonesia [20], which is relevant to designing a more permanent monitoring network along the Mangottong corridor.

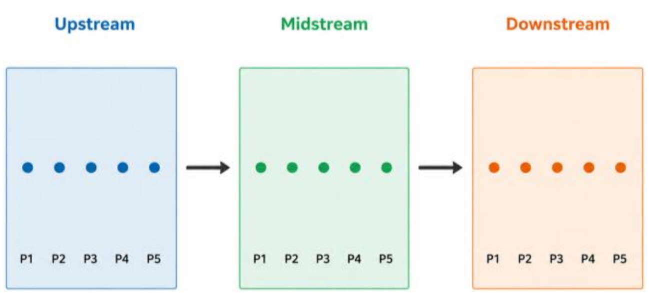

Figure 1. Schematic longitudinal sampling design: three river sections and five observations (P1–P5) per section.
Source: authors' field dataset.

3. Results and Discussion

3.1 Longitudinal hydraulic and concentration patterns

Summed water discharge increased monotonically along the sampled corridor (Table 1). The upstream section carried 5.178 $m^3\ s^{-1}$, the midstream section 7.554 $m^3\ s^{-1}$, and the downstream section 8.438 $m^3\ s^{-1}$. The midstream total was 45.9% above the upstream value, and the downstream total was 62.9% above upstream. Pointwise discharge was heterogeneous at every section (Figure 2). P4 carried the highest discharge at all three cross-sections, reaching 1.616, 2.460, and 2.839 $m^3\ s^{-1}$ upstream, midstream, and downstream, respectively. The mean point discharge increased from 1.036 ± 0.471 to 1.511 ± 0.672 and 1.688 ± 0.848 $m^3\ s^{-1}$. Coefficients of variation were 45.4%, 44.5%, and 50.2%, showing that the distribution of conveyance remained uneven across the channel.

SSC did not follow the same longitudinal pattern as discharge. The arithmetic mean was 533.3 mg L^{-1} upstream and 540.0 mg L^{-1} midstream, but increased to 1,733.2 mg L^{-1} downstream. The upstream section ranged from 200.0 to 1,133.3 mg L^{-1}, the midstream section from 400.0 to 666.6 mg L^{-1}, and the downstream section from 533.3 to 2,800.0 mg L^{-1} (Figure 3). The downstream cross-section was therefore both more sediment-rich and strongly heterogeneous. P3 had a concentration close to the midstream range, whereas P4 and P5 exceeded 2,600 mg L^{-1}.

Discharge weighting sharpened this contrast. Section-weighted SSC was 626.5 mg L^{-1} upstream, 568.3 mg L^{-1} midstream, and 1,829.2 mg L^{-1} downstream. The midstream value was 9.3% lower than upstream, but downstream weighted SSC was 221.9% higher than midstream and 2.92 times the upstream value. The Kruskal–Wallis test indicated an overall longitudinal difference in point SSC ($H = 6.54$, $p = 0.038$; $\eta^2 H \approx 0.38$). Holm-adjusted pairwise comparisons did not remain significant (adjusted $p \geq 0.095$), so the inferential result should be treated as evidence of a reach-scale pattern rather than proof of a stable population difference. The descriptive contrast, particularly the high downstream concentrations, is more informative for this small spatial sample.

Table 1. Reach-scale hydraulic and suspended-sediment metrics

Reach	ΣQ ($m^3\ s^{-1}$)	Mean Q ± SD ($m^3\ s^{-1}$)	Mean SSC ± SD (mg L^{-1})	Q-weighted SSC (mg L^{-1})	Σ load (t d^{-1})	Dominant point (% load)
Upstream	5.178	1.036 ± 0.471	533.3 ± 371.2	626.5	280.3	P4 (56.5%)
Midstream	7.554	1.511 ± 0.672	540.0 ± 111.5	568.3	370.9	P4 (36.3%)
Downstream	8.438	1.688 ± 0.848	1,733.2 ± 971.9	1,829.2	1,333.5	P4 (49.0%)

Note. Q-weighted SSC = $\Sigma(Q_i C_i)/\Sigma Q_i$. Integrated suspended load = $\Sigma(0.0864 Q_i C_i)$.

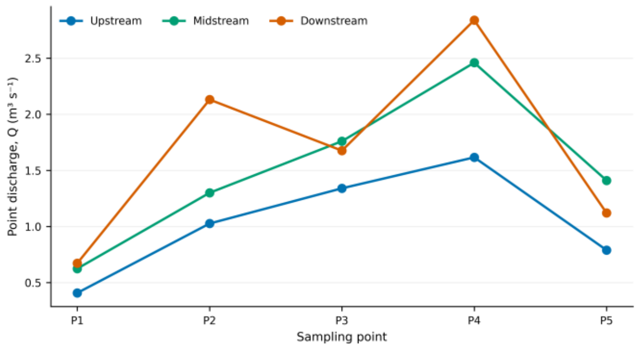

Figure 2. Pointwise water-discharge profiles at the upstream, midstream, and downstream sections.

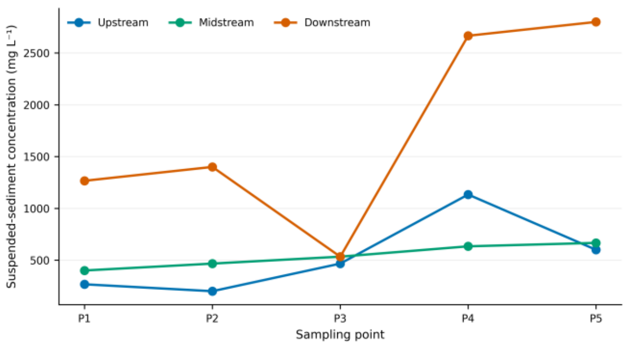

Figure 3. Pointwise suspended-sediment concentration profiles across the three sections.

3.2 Downstream amplification of suspended-sediment flux

The strongest result emerged when discharge and SSC were combined. Integrated instantaneous suspended load was 280.3 t d^{-1} upstream, 370.9 t d^{-1} midstream, and 1,333.5 t d^{-1} downstream (Figure 4). The downstream section carried 4.76 times the upstream load while water discharge increased only 1.63-fold. If additional water were the principal explanation, the load ratio would be expected to track the discharge ratio more closely. Instead, most of the amplification arose because the lower reach carried substantially more sediment per unit volume of water.

The point-load distribution further illustrates why integrated flux provides a more informative reach-scale metric than concentration alone. Upstream, the highest concentration and the highest discharge both occurred at P4, causing a pronounced load concentration at that point. Midstream, SSC varied less across the section, so transport was distributed more evenly even though P4 remained hydraulically dominant. Downstream, the two controls converged again: P4 combined the largest discharge with the second-highest SSC, while P5 combined the highest SSC with a smaller discharge. The result is a section in which one point dominates mass transport but adjacent points still make substantial contributions. This spatial structure would be lost if the section were represented by a single average concentration.

This divergence is consistent with evidence from larger regulated and free-flowing systems where water and sediment regimes remain coupled but change by different magnitudes. Long-term Pearl River records show that sediment load can evolve differently from water discharge [21], while dam-affected rivers in the Narmada and Red River systems exhibit substantial changes in sediment transport that are not captured by discharge alone [22,23]. Effective-discharge analysis in the Upper Narmada likewise shows that the flow classes responsible for most suspended transport can shift after regulation [24]. Estuarine modelling also demonstrates that longitudinal SSC and sediment flux may change direction or magnitude across hydraulic transition zones [25]. These studies differ greatly in scale from the Mangottong River, but they support the same analytical separation between water quantity and transported sediment mass.

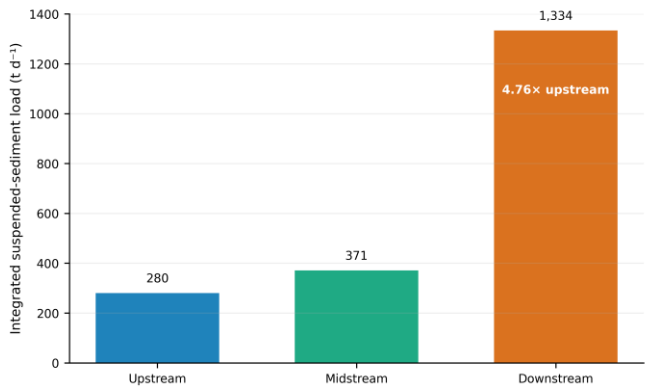

Figure 4. Integrated instantaneous suspended-sediment load by section.

3.3 Cross-sectional heterogeneity and sediment supply

Lateral heterogeneity was equally important. Upstream P4 contributed 158.2 t d^{-1}, or 56.5% of the section load. Midstream P4 contributed 134.6 t d^{-1}, or 36.3%, while downstream P4 contributed 654.1 t d^{-1}, equivalent to 49.0% of the downstream total. Downstream P5 had the highest concentration (2,800 mg L^{-1}) but a smaller discharge than P4, so its load was 271.0 t d^{-1}. A single grab sample at P3 would have suggested a downstream SSC of only 533.3 mg L^{-1}, whereas P5 would have suggested 2,800 mg L^{-1}. Neither point alone would have represented the section.

Such cross-sectional asymmetry has been observed in river and estuarine settings where secondary circulation, bathymetry, confluence mixing, or tidal processes redistribute suspended material. Hyperspectral observations at a river confluence show that mixing patterns can be strongly non-uniform [26], and lateral mixing asymmetry has been linked to longitudinal sediment transport in estuarine turbidity maxima [27]. Indonesian measurements in Kali Wonokromo similarly document spatially variable flow and suspended-sediment patterns in a meandering, tide-affected channel [6]. The Mangottong data therefore support a practical sampling recommendation: concentration measurements should be paired with the local discharge they represent, and the main conveyance core should not be assumed to coincide with a single geometric centreline.

The distribution of SSC also provides clues about sediment supply. Midstream concentrations were relatively uniform, with a coefficient of variation of 20.7%, whereas upstream and downstream SSC had coefficients of variation of 69.6% and 56.1%. The lower reach may therefore have received localized sediment inputs, remobilized stored fine material, or contained incomplete lateral mixing during sampling. Stream-corridor studies show that banks and stored channel sediment can account for a substantial share of downstream suspended load [8], while tributary measurements demonstrate that small lateral sources can materially alter the receiving-river sediment budget [9]. In agricultural systems, drainage collectors can also supply cohesive sediment to the main river [28].

The data do not allow these mechanisms to be separated. A net load gain of approximately 1,053.2 t d^{-1} between the upstream and downstream sections is dimensionally meaningful, but it cannot be assigned uniquely to bank erosion, bed remobilisation, tributary supply, or temporal mismatch. Event-scale studies show that apparent storage environments can export sediment when previously deposited material is reworked [29], and extended sediment-rating formulations improve predictions when storage and anthropogenic sources are represented explicitly [30]. The present dataset lacks synchronized tributary sampling, bed-material tracing, bank-erosion surveys, and continuous hydrographs, so source attribution remains a hypothesis for future work.

The magnitude of the load values also requires careful interpretation. The conversion 0.0864CQ yields tonnes per day when C is expressed in mg L^{-1} and Q in $m^3 s^{-1}$. The high downstream value therefore follows directly from the combination of discharge and measured SSC; it is not a consequence of annualisation. At the same time, the measurement window does not establish how long this condition persisted. A short-lived high-SSC state can generate a large instantaneous load without implying a similarly high daily or annual mean. This distinction is critical in rivers where storm events carry a disproportionate fraction of sediment, as shown by long-term and event-based monitoring [1,31]. The load values should therefore be read as comparable snapshots across the three sections rather than as annual sediment-yield estimates. The point-level discharge, SSC, and recalculated suspended-sediment loads summarized in Table 2 further illustrate the pronounced cross-sectional variability, particularly at the downstream section.

Table 2. Point-level discharge, SSC, and recalculated suspended-sediment load

Reach	Point	Q ($m^3 s^{-1}$)	SSC (mg L^{-1})	Suspended load (t d^{-1})
Upstream	P1	0.407	266.6	9.4
Upstream	P2	1.026	200.0	17.7
Upstream	P3	1.340	466.6	54.0
Upstream	P4	1.616	1,133.3	158.2
Upstream	P5	0.789	600.0	40.9
Midstream	P1	0.624	400.0	21.6
Midstream	P2	1.300	466.6	52.4
Midstream	P3	1.760	533.3	81.1
Midstream	P4	2.460	633.3	134.6
Midstream	P5	1.410	666.6	81.2
Downstream	P1	0.672	1,266.0	73.5
Downstream	P2	2.131	1,400.0	257.8
Downstream	P3	1.676	533.3	77.2
Downstream	P4	2.839	2,666.6	654.1
Downstream	P5	1.120	2,800.0	271.0

Statistical summary: SSC Kruskal–Wallis H = 6.54, p = 0.038; Holm-adjusted pairwise p ≥ 0.095. Point load H = 5.18, p = 0.075. Q–SSC Spearman ρ = 0.476, p = 0.073.

3.4 Interpretation of sedimentation and management implications

The moderate Spearman association between point discharge and SSC (ρ = 0.476, p = 0.073) reinforces this interpretation. Higher-discharge points often carried more suspended material, but the relation was not monotonic. Downstream P3 carried 1.676 $m^3 s^{-1}$ at 533.3 mg L^{-1}, whereas P5 carried only 1.120 $m^3 s^{-1}$ at 2,800 mg L^{-1}. Hydraulics therefore influenced transport without fully determining concentration. By contrast, discharge and calculated point load were strongly correlated (ρ = 0.768, $p < 0.001$), which is expected because discharge is a multiplicative term in the load calculation and should not be interpreted as independent causal evidence.

The findings also clarify the meaning of sedimentation. Subtracting an upstream concentration from a downstream concentration does not yield a sedimentation rate because concentration is not a mass flux and because water discharge differs among sections. Sedimentation requires evidence of storage within a defined control volume. The present measurements instead indicate that more suspended sediment was moving through the lower section during the sampled state. Studies based on repeated monitoring show that reliable sediment budgets require synchronized inflow and outflow estimates together with uncertainty bounds, particularly when transport is dominated by events [31]. Hydrosedimentary responses can also change sharply between flow states and basins [32], which is why the Mangottong loads should not be extrapolated to annual yield.

From a management perspective, the lower reach deserves priority for repeated monitoring because it combined the largest discharge, the highest discharge-weighted SSC, and the highest suspended load. However, a transport hotspot is not automatically a deposition hotspot. Deposition occurs where incoming sediment exceeds the local capacity to keep particles in motion. Numerical work on river mouths shows how fluvial water and sediment supply can interact with coastal hydrodynamics to generate substantial accumulation or closure [33], and catchment-to-coast observations demonstrate that suspended sediment can remain dynamically important through nearshore environments [34]. The Mangottong survey did not measure bathymetric change at the river mouth, so shoaling remains a management concern rather than a demonstrated outcome of this dataset.

For river engineering, the observed downstream enrichment has two implications. First, a hydraulic design based solely on water discharge could underestimate the sediment burden passing through the lower reach. Second, a sediment-control measure placed without identifying the source of the added load could simply shift erosion or deposition elsewhere. The appropriate sequence is therefore diagnostic before structural: establish repeated section fluxes, identify tributary and bank contributions, determine where channel storage changes, and only then evaluate whether flow-control, bank protection, sediment trapping, or maintenance dredging is justified. This approach is consistent with recent studies that treat sediment management as a coupled hydrological and morphological problem rather than a single-parameter design task [32,35].

Hydraulic interventions can alter retention and scour by changing local velocity and residence time. In a recent Jurnal Linears study on the Krueng Aceh River, added hydraulic resistance from water hyacinth reduced flow velocity and increased residence time under the tested conditions, thereby favouring particle retention [36]. Laboratory studies in the target engineering literature likewise show that porous flow-control structures can reduce local velocity and scour [18,19]. These results should not be transferred directly to the Mangottong River as design prescriptions, but they illustrate the hydraulic sensitivity of sediment retention and support testing site-specific, low-impact flow-management measures only after the dominant sediment sources and flood-conveyance requirements are resolved.

A practical monitoring programme should combine repeated multi-point cross-sections with continuous or event-triggered measurements. Optical surrogate methods can capture rapid SSC variability when calibrated against physical samples [14], and high-frequency radiometry demonstrates how much short-lived sediment variability can be missed by sparse sampling [13]. Sampling should cover low flow, rainfall-driven rising stages, peak flow, and recession. Rainfall and stage records should be synchronized with SSC, while tributary inflows, bank condition, bed texture, and cross-sectional geometry should be documented between the three sections. Morphodynamic modelling under extreme rainfall has shown the value of combining hydraulic and sediment information when evaluating channel change [35].

3.5 Limitations and monitoring priorities

The study has three main limitations. First, the measurements represent a limited field campaign rather than repeated hydrologic events, so temporal persistence cannot be assessed. Second, some intermediate field calculations were inconsistent, requiring the analysis to rely on the final point discharges and laboratory SSC values that could be verified directly. Third, the study addresses suspended load only; bed load and changes in channel storage were not measured. These limitations narrow the inference but do not remove the central observation: during the surveyed state, sediment flux increased much more rapidly downstream than water discharge. Future work should test whether this disproportionate amplification persists across seasons and should identify whether the lower-reach enrichment is supplied primarily by banks, bed storage, lateral inflows, or combinations of these sources.

4. Conclusion

The Mangottong River measurements show a clear mismatch between longitudinal changes in water discharge and suspended-sediment transport. Section discharge increased from 5.178 $m^3\ s^{-1}$ upstream to 7.554 $m^3\ s^{-1}$ midstream and 8.438 $m^3\ s^{-1}$ downstream. Discharge-weighted SSC changed from 626.5 to 568.3 and 1,829.2 mg L^{-1}, while suspended load increased from 280.3 to 370.9 and 1,333.5 t d^{-1}. The downstream section therefore carried 4.76 times the upstream suspended load despite only a 1.63-fold increase in water discharge.

The result indicates that sediment enrichment, rather than discharge growth alone, controlled the observed downstream amplification. The lower cross-section was also strongly heterogeneous: P4 carried 49% of the downstream load because high discharge coincided with a high SSC. This pattern demonstrates why isolated concentration samples can misrepresent section transport and why discharge-weighted measurements are preferable for sparse surveys.

The calculated loads describe the sampled state and should not be interpreted as annual sediment yield or net deposition. Establishing a true sediment budget will require repeated event-based measurements, tributary accounting, bed-load observations, and evidence of storage change. For management, the lower reach is the priority location for monitoring, while any sediment-control intervention should be preceded by source identification and an assessment of its effect on flood conveyance.

Declaration of generative AI and AI-assisted technologies in the manuscript preparation process

During the preparation of this work, OpenAI ChatGPT was used to support manuscript organization, language refinement, and the presentation of calculations derived from the study data. All authors subsequently reviewed and edited the manuscript and independently verified the data, calculations, references, interpretations, and scientific conclusions. The authors take full responsibility for the accuracy, integrity, and content of the published work.

CRediT authorship contribution statement

Muhammad Scyroth Arianto and **Ilfan Muis**: Conceptualization, Methodology, Investigation, Data curation, Formal analysis, Visualization, Writing – original draft, Writing – review & editing. **Andi Makbul Syamsuri**: Investigation, Data curation, Validation, Resources, Writing – review & editing. **Fithriyah Arief Wangsa**: Methodology, Validation, Supervision, Project administration, Writing – review & editing.

Funding

This research received no specific grant from funding agencies in the public, commercial, or not-for-profit sectors.

Declaration of competing interest

The authors declare that they have no known competing financial interests or personal relationships that could have appeared to influence the work reported in this paper.

Data availability

All numerical data supporting the findings of this study are presented within the manuscript, tables, and figures. Additional information related to the field measurements may be made available by the corresponding author upon reasonable request.

References

[1] Battaglin WA, Kisfalusi ZD. Characterization of and Relations Among Precipitation, Streamflow, Suspended-Sediment, and Water-Quality Data at the U.S. Army Garrison Fort Carson and

Piñon Canyon Maneuver Site, Colorado, Water Years 2016–18. 2022.
[2] Skålevåg A, Korup O, Bronstert A. Inferring sediment-discharge event types in an Alpine catchment from sub-daily time series. Hydrology and Earth System Sciences. 2024;28(20):4771-96.
[3] Bezak N, Lebar K, Bai Y, Rusjan S. Using Machine Learning to Predict Suspended Sediment Transport under Climate Change. Water Resources Management. 2025;39(7):3311-26.
[4] Borella DR, de Souza AP, de Almeida FT, de Abreu DC, Hoshide AK, Carvalho GA, et al. Dynamics of Sediment Transport in the Teles Pires River Basin in the Cerrado-Amazon, Brazil. Sustainability (Switzerland). 2022;14(23).
[5] Bui TTP, Kantoush S, Kawamura A, Du TLT, Bui NT, Capell R, et al. Reservoir operation impacts on streamflow and sediment dynamics in the transboundary river basin, Vietnam. Hydrological Processes. 2023;37(9).
[6] Patriadi A, Pattiraja AH, Sukmara RB, Wahab MF. Assessing Flow, Sediment, and Salinity Patterns in Tidal-Affected Meandering Rivers: Insights from Kali Wonokromo. International Journal on Advanced Science, Engineering and Information Technology. 2024;14(4):1488-95.
[7] Erwanto Z, Lasminto U, Iranata D, Maulana MA. Hydrometric sensor-based monitoring and empirical modeling of sediment transport and river erosion dynamics in a bird feather-type watershed. Journal of Engineering and Applied Science. 2026;73(1).
[8] Blount JD, Lenoch LEK, Fitzpatrick FA. Stream corridor and upland sources of fluvial sediment and phosphorus from a mixed urban-agricultural tributary to the Great Lakes. Journal of Great Lakes Research. 2022;48(6):1536-49.
[9] Haught DRW, Marineau MD, Minear JT, Wright SA, Lopez JV. Sediment Transport in Two Tributaries to the San Joaquin River Immediately Below Friant Dam—Cottonwood Creek and Little Dry Creek, California. 2023.
[10] Rosas MA, Viveen W, Vanacker V. Spatial variation in specific sediment yield along the Peruvian western Andes. Catena. 2023;220.
[11] Chalov S, Denisova I, Moreido V, Solonikov I, Loshkov O, Botavin D, et al. Streamflow and sediment dynamics affected by precipitation events and land use changes in the heavily urbanized small catchment of Moscow megacity. Urban Climate. 2026;65.
[12] Rahim MA, Liu S, Hu K, Li H, Islam M, Hossain S. Revealing inconsistency of the sediment-water relationships in the Brahmaputra River: A comparative analysis of upstream and downstream cross-sections. Journal of Mountain Science. 2025;22(8):2819-36.
[13] Borges HD, Martinez JM, Harmel T, Cicerelli RE, Olivetti D, Roig HL. Continuous Monitoring of Suspended Particulate Matter in Tropical Inland Waters by High-Frequency, Above-Water Radiometry. Sensors. 2022;22(22).
[14] Vas L, Tamás EA. Surrogate Method for Suspended Sediment Concentration Monitoring on the Alluvial Reach of the River Danube (Baja, Hungary). Applied Sciences (Switzerland). 2023;13(10).
[15] Efthimiou N. Suspended Load Estimation in Data Scarce Rivers. Water Resources Management. 2025;39(1):311-78.
[16] Salarijazi M, Modabber-Azizi S, Mohammadi M, Mohammadrezapour O, Ghorbani K. Temporal Classification to Improve the Precision of Suspended Sediment Rating Curve (Case Study: Gorganrood Basin). Iranian Journal of Science and Technology - Transactions of Civil Engineering. 2025;49(4):4051-62.
[17] Yusuf M, Tongeng AB, Marupah M, Latif S. Analisis Eksperimental Pengaruh Sabo Dam Tipe Beam terhadap Karakteristik Aliran Debris pada Variasi Kemiringan Saluran. Journal of Green Complex Engineering. 2026;3(2):67-72.
[18] Baharuddin A, Karim N, Ali MY, Latif S. Investigasi Eksperimental Pengendalian Gerusan Pilar Jembatan Menggunakan Deflektor Arus Bawah Air Berpori. Journal of Green Complex Engineering. 2026;3(2):83-94.
[19] Ali A, Karim N, Syamsuri AM, Latif S. Efektivitas Deflektor Silinder Pori Bertulang dalam Mengendalikan Aliran di Sekitar Pilar Jembatan. Journal of Green Complex Engineering. 2026;3(2):95-102.
[20] Ajami FM, Bahrun RS, Indrayani AF, Ikram F. Integrasi Analisis Kerentanan dan Desain Bangunan Ukur dalam Mitigasi Banjir Skala Desa. Jurnal Linears. 2026;9(1):51-9.
[21] Liu Z, Fagherazzi S, Liu X, Shao D, Miao C, Cai Y, et al. Long-term variations in water discharge and sediment load of the Pearl River Estuary: Implications for sustainable development of the Greater Bay Area. Frontiers in Marine Science. 2022;9.
[22] Prajapati P, Meena GK, Swarnkar S, Jha SK. Impact of Indira Sagar Dam on Water Discharge and Sediment Flow Regimes of the Narmada Basin. Journal of Hydrologic Engineering. 2025;30(2).
[23] Quang NH, Viet TQ. Long-term analysis of sediment load changes in the Red River system (Vietnam) due to dam-reservoirs. Journal of Hydro-Environment Research. 2023;51:48-66.
[24] Dixit S, Timbadiya PV, Patel PL. Effective discharge for suspended sediment transport in the pre- and post-dam scenarios in the Upper Narmada River, India. ISH Journal of Hydraulic Engineering. 2026;32(1):77-96.
[25] Chen W, Ban H, Mao C, Liang H, Jiang M. Sediment Dynamics Subject to Sea Level Rise in the Yangtze River Estuary. Journal of Ocean University of China. 2024;23(6):1572-82.
[26] Kwon S, Seo IW, Lyu S. Investigating mixing patterns of suspended sediment in a river confluence using high-resolution hyperspectral imagery. Journal of Hydrology. 2023;620.
[27] Teng L, Cheng H, Zhang E, Wang Y. Lateral Variation of Tidal Mixing Asymmetry and Its Impact on the Longitudinal Sediment Transport in Turbidity Maximum Zone of Salt Wedge Estuary. Journal of Marine Science and Engineering. 2022;10(7).
[28] Cancio NCO, Pierini JO. Suspended sediment transport in Rio Colorado agricultural basin, Argentina. Frontiers in Built Environment. 2023;9.
[29] De Freitas CR, Grenfell S. Event-scale suspended sediment fluxes in a dryland environment valley-bottom wetland: Implications for downstream sediment and phosphorous fluxes. Geomorphology. 2024;452.
[30] Wolf S, Stenger D, Steudtner F, Esser V, Lehmkuhl F, Schüttrumpf H. Modeling anthropogenic affected sediment transport in a mid-sized European river catchment–extension of the sediment rating curve equation. Modeling Earth Systems and Environment. 2023;9(4):3815-35.
[31] Kramer Stajnko J, Jecl R, Nekrep Perc M. Advances in Monitoring and Understanding the Dynamics of Suspended-Sediment Transport in the River Drava, Slovenia: An Analysis More than a Decade-Long. Applied Sciences (Switzerland). 2023;13(15).
[32] Ouakhir H, Ennaji N, Goumih M, Ghachi ME, Barhazi L, Hilali A, et al. Hydrosedimentary Response of the Two River Basins from Middle and High Atlas of Morocco: A Multiscale and Systematic Approach. Earth Systems and Environment. 2025.
[33] Aouiche I, Sedrati M, Anthony EJ. Modelling of Sediment Transport and Deposition in Generating River-Mouth Closure: Oum-Errabia River, Morocco. Journal of Marine Science and Engineering. 2023;11(11).
[34] Santhikrishnan S, Jyothibabu R, Sajeev R, Vishnu CB, Albin KJ, Alok KT, Pandiya Rajan RS. Impact of river discharge and suspended sediments on the nearshore benthic environment along the Indian southwest coast. Science of the Total Environment. 2024;954.
[35] Tunas IG, Harsanto P, Arafat Y. Modeling Bed Morphology Evolution in an Alluvial River under Extreme Rainfall Using a 2D Hydrodynamic–Sediment Transport Approach. International Journal of Computational Methods and Experimental Measurements. 2025;13(3):667-79.
[36] Akmal A, Munawir M, Puteh MAF, Syauqi TM, Saputra H. Hydrological Assessment of A Water Hyacinth (Eichhornia crassipes) Filtration System for Microplastic and Water Quality Improvement in The Krueng Aceh River. Jurnal Linears. 2026;9(1):9-18.

This page is intentionally left blank.

Journal of Green Complex Engineering